Supporting Online Material for

Counting Low–Copy-Number Proteins in a Single Cell

Bo Huang, Hongkai Wu, Devaki Bhaya, Arthur Grossman, Sebastien Granier, Brian K. Kobilka, Richard N. Zare*

*To whom correspondence should be addressed. E-mail: zare@stanford.edu

This PDF file includes:

Materials and Methods
Figs. S1 to S6
Table S1
References

Other Supporting Online Material for this manuscript includes the following: (available at www.sciencemag.org/cgi/content/full/315/5808/81/DC1)

Movies S1 and S2

Counting Low-Copy-Number Proteins in a Single Cell

Bo Huang, Hongkai Wu, Devaki Bhaya, Arthur Grossman,

Sebastien Granier, Brian K. Kobilka, Richard N. Zare[*]

Supporting Information

1. Microfluidic chip fabrication

Polydimethylsiloxane (PDMS) microfluidic devices are fabricated in the Stanford Nanofabrication Facilities with standard soft photolithography similar to the process described previously (*S1*). The photolithography masks are designed with Freehand 10 (Macromedia) and printed on a transparency film with a high-resolution (3600 dpi) printer (Media Morphosis). To produce the silicon masters for the molecule counting chips, we first make the molecule counting section from a thin layer (~ 2 µm) of negative photoresist (SU-8 2002, MicroChem). The rest of the channels are then fabricated with a 15 µm (insect cell analysis chip) or 7 µm (cyanobacteria analysis chips) layer of positive photoresist (SPR 220-7). The masters for the channel layer in valve-controlled chips are heated to 115 °C for 30 min to reflow the positive photoresist so that the channels form a smooth, round shape. The masters for the control layer of these chips are made of 40 µm thick negative photoresist (SU-8 50, MicroChem). Photoresist exposure is performed on a contact aligner (Electronic Vision 620, EV Group). The heights of the channels are measured with a surface profiler (DekTak, Veeco). The developed silicon master is treated with perfluoro-1,1,2,2-tetrahydrooctyltrichlorosilane vapor (United Chemical

Technologies) in a vacuum desiccator to prevent adhesion of PDMS during the molding procedure.

The microfluidic chips are cured from PDMS prepolymer (RTV 615A and 615B, purchased from General Electric, mixed with 10:1 mass ratio) or its mixture with cyclohexane (as a thinner for spin coating). For a valve-controlled chip, the top layer (control layer) is formed by pouring mixed PDMS prepolymer on the silicon master, degassing, followed by curing at 70 °C for 30 min. After the cured PDMS piece is peeled off the master, holes are punched to connect to the pressure controller. The second layer (channel layer) is formed by spin coating a mixture of PDMS prepolymer with cyclohexane (2:1 mass ratio for insect cell analysis chips and 1:1.3 for cyanobacteria analysis chips; spin coating at 500 rpm for 18 s and then 1500 rpm for 60 s) onto the channel master and partially curing at 70 °C for 9 min. The control layer is then aligned and attached to the channel layer. More PDMS prepolymer is added to cover the silicon wafer. After curing at 70 °C for 30 min, the two layers are bonded together. The PDMS piece is peeled from the master and holes are punched to form the reagent inlets and outlets. The bottom layer is created by spin coating a mixture of PDMS prepolymer with cyclohexane (1:2 mass ratio, spin coating at 900 rpm for 9 s and then 2000 rpm for 30 s) on a microscope coverglass and curing at 70 °C for 20 min. The thickness of this PDMS layer is about 10 µm, which is required for the use of high numerical aperture objectives. The microfluidic chip is assembled by placing the PDMS piece bearing the channels on the PDMS-coated coverglass. For cyanobacteria analysis chip and "double-T" chips, short glass tubes are glued to the holes as reservoirs. The assembled PDMS chip is baked

at 115 °C for 30 min to bond the channel layer to the bottom layer. "Double-T" chips that do not have the valve layer are fabricated in a similar way, without the final 115 °C baking step.

2. Optical setup and the performance of the cylindrical optics

The separation and imaging experiments are performed on a Nikon TE2000-U inverted microscope. The excitation sources are a 532-nm diode-pumped frequency-doubled Nd:YAG laser (Compass 215M, Coherent) and a 638-nm diode laser (RCL-638-25, Crystalaser), which are combined and coupled to the same single-mode optical fiber. The laser beam emerging from the optical fiber is collimated with a 100 mm achromatic lens, shaped by a 1 cm × 1 cm square hole, and sent into the microscope through a spherical or cylindrical lens (each having a focal length of 400 mm). Fig. S1A shows the formation of a curtain-shaped laser focus in the microchannel by the combination of the cylindrical lens and the microscope objective. The emitted fluorescence is collected by the microscope objective and filtered by a dichroic mirror (400-535-635 TBDR, Omega Optical) and a band pass filter (HQ675/50m, Chroma). For laser induced fluorescence detection of capillary electrophoresis separation, the cylindrical lens is used for excitation, and a photon counting photomultiplier tube module (H6240-01, Hamamatsu) is used for detection, with a 50 μm slit installed at the microscope image plane to reject the out-of-focus emission. For wide-field fluorescence imaging and molecule counting, an intensified CCD camera (I-Pentamax, Roper Scientific) serves as the detector. In

molecule counting experiments, the power of the laser beam emerging from the objective is about 10 mW, and the line-shaped laser focus at the sample is 50 μm long.

By imaging the fluorescence from a glass surface coated with Atto 565 labeled streptavidin (Sigma Aldrich), we can compare the z-dependence of the excitation laser strength in three different configurations: (a) wide-field, in which a spherical lens focuses the excitation laser beam to the back focal point of the microscope objective (Nikon Plan Apo 100× oil NA 1.4), (b) cylindrical, in which a cylindrical lens focuses the laser beam to the back focal plane of the objective, and (c) confocal, in which a parallel laser beam is sent into the objective. Fig. S1B shows that the confocal configuration has the sharpest drop in excitation strength when the imaging plane moves away from the focal plane, the cylindrical configuration shows similar but slightly lower z-resolution, and the wide-field configuration has almost constant excitation strength when the z position of the sample changes. A 2 μm channel fits well into the focus of the cylindrical configuration and the out-of-focus background is suppressed.

3. Molecule counting algorithm

When a fluorescent molecule travels across the excitation laser focus, its fluorescence is recorded by the intensified CCD camera as a bright spot in the image. We record flashes rather than tracks because the motion of the molecules through the detection curtain is faster than the time resolution of the CCD camera. During the CCD integration time (50 ms or 20ms), multiple analyte molecules can pass the detection curtain. At a relatively low concentration, the resultant fluorescent spots are likely to

appear at different locations along a line that corresponds to the position of the detection region (Fig. 1C, *x* direction). To identify the number of target molecules in a certain frame of the CCD image, we first use a Fourier low-pass filter to reduce the noise in the image. Continuous regions that are above a set threshold are marked. These regions are considered to be the signal from a fluorescent molecule if the following two criteria are satisfied: (1) the area of a region is larger than 15 pixels (0.76 μm^2), and (2) the coordinates of the center-of-mass of a region are within the range of the detection curtain.

When the analyte concentration increases, more molecules are recorded in each image frame, thus increasing the probability of having two or more fluorescent spots very close together. Because each of these spots have a finite size (mainly determined by diffraction and their distance from the focal plane of the objective), when we apply the threshold, they are marked as one continuous region. Therefore, after the threshold is applied, we examine the cross-section of the image along the detection curtain (Fig. S2A). By identifying local maxima and minima in the cross-section, we can resolve closely spaced molecules.

Another source of bias in counting is the possibility that one molecule is imaged in two consecutive frames. In our slow-flow method, the time for a molecule to travel across a 1 μm wide detection region is about 2 ms; therefore, if a molecule reaches the detection region at the end of one CCD integration period, it could be recorded in the next integration period as well (the time interval between two frames is shorter than 1 ms

in our intensified CCD camera). Because the Brownian motion of the molecule within this 2 ms time is not significant (comparable to the diffraction-limited laser spot size), we expect this molecule to appear at the same x positions in the two frames. Therefore, after the fluorescent spots are counted in one image frame, the x positions of their centers-of-mass are compared to those in the previous frame. If the difference is within 2 pixels (450 nm), the fluorescent spot in the second frame is marked as an invalid count (Fig. S2B).

Despite these efforts to compensate for biases in molecule counting, the chance of false negatives increases when the number of molecules in each frame is very high (>10 molecules per frame). A solution is to increase the length of the separation channel, which increases the peak width when the analyte reaches the detection point. By this means, the molecules are spread into more image frames, so that the number of molecules per frame is controlled.

4. The counting efficiency of Alexa Fluor 647 labeled streptavidin

We use a standard "double-T" microfluidic chip (see Fig. S3A) with rectangular channels to perform the molecule counting of Alexa Fluor 647 labeled streptavidin (A647-SA, purchased from Invitrogen). The concentration of A647-SA stock solution is calculated by measuring the absorbance of the protein and the dye at 280 nm and subtracting from it the contribution from the dye, determined by measuring its absorption at 647 nm. The separation buffer contains 20 mM HEPES (pH 7.5), 0.1 wt% N-dodecyl-β-D -maltoside (DDM, from AnaTrace), and 0.05 wt% sodium dodecylsulfate (SDS,

from Sigma-Aldrich). The separation uses electric field strengths of about 300 V/cm. A647-SA can be separated into multiple peaks using capillary zone electrophoresis and laser induced fluorescence detection (Fig. S3C). These peaks can be attributed to the charge ladder created when different numbers of negatively charged dyes are labeled on the streptavidin molecule (*S2*). By inserting a short (10 μm long) molecule counting section into the separation channel, we resolve this charge ladder using molecule counting at a low sample concentration (Fig. S3D).

We measure the size of the injection plug by imaging the injection procedure at the "double-T" junction using 200 nM A647-SA as the sample (Fig. S3B). An effective plug area is obtained by dividing the integrated intensity of the injection plug with the intensity in the channels filled with sample solution during the loading step. The injection plug volume is derived by multiplying this area by the thickness of the channel (7.6 μm). From five different measurements, we calculate that the effective size of the injection plug is 35 ± 4 pL, which corresponds to 1557 ± 174 injected A647-SA molecules when the sample concentration is 73 pM.

The molecule counting efficiency depends on the threshold chosen for the image analysis. A lower threshold decreases the probability of false negatives in counting but increases that of false positives from background noise. To characterize this effect, we analyze the total molecule counts from the same experiment (900 frames) with different thresholds. The molecule counts in a blank experiment (no sample is injected) are

calculated in the same way. As seen in Fig. S4A, a threshold lower than 25 introduces significant false counts from background noise. Using a threshold of 30, the count from seventeen counting experiments is 929 ± 43 molecules (after subtracting the counts from blank experiments). Therefore, the corresponding overall counting efficiency for streptavidin molecules that have different degrees of labeling is about 60%.

Two factors can contribute to the incomplete counting of sample molecules: missed molecules in identification (identification efficiency) and loss in transportation from the sample reservoir to the detection point (transportation efficiency). We measure the transportation efficiency by performing the counting experiment on a "double-T" chip that moves the detection point from 5 mm to 20 mm after the injection junction. Such experiments with the same A647-SA sample give an overall molecule counts of 961 ± 22 (the threshold is 30, blank control is subtracted, and the difference in injected sample concentration cause by different sample loading times is corrected for), indicating that the transportation efficiency of a 15 mm channel is nearly 100% and contributes very little to the loss in counting efficiency. Therefore, we can assume that the counting efficiency is fully determined by the identification efficiency in the image analysis.

From the threshold analysis, we can actually estimate the true sample molecule counts directly. Although all molecules of the same kind have the same photophysical parameters, they show different fluorescence intensities because they are at different positions in the channel which have different excitation laser intensity. Molecules distant

from the focal plane are dimmer also because their images are blurred by defocusing. A higher threshold is likely to reject more of these dim molecules. We can analyze the same set of images using different thresholds (higher than the level at which background noise starts to mix with the fluorescence signal) and interpolate the molecule counts to a threshold of zero (which hypothetically should not reject any fluorescence signal) to estimate the true molecule number. In Fig. S4A, a simple linear interpolation using the molecule counts with the threshold between 25 and 50 gives a molecule count of 1591 $\pm$ 60, which is close to the actual number. We have found that this estimation method is applicable to the major species in our single-cell analysis (Fig. S4B). More sophisticated modeling could provide higher accuracy in estimating the true molecule counts.

5. Analysis of β_2AR in SF9 cells

SF9 insect cells were grown at 27°C in suspension cultures in ESF-921 medium (Expression Systems, CA) supplemented with 0.5 mg/mL gentamicin. Recombinant baculoviruses of the human β_2AR epitope-tagged at the amino-terminus with the cleavable influenza-hemagglutinin signal sequence followed by the FLAG epitope and at the carboxyl-terminus with six histidines were generated in SF9 cells using the Bac-to-Bac® Baculovirus Expression System (Invitrogen). SF9 cell cultures were infected at a density of $\sim 2 \times 10^6$ cells/ml and used for experiments after 18 hr of infection.

To measure the average copy number of β_2AR by anti-FLAG M1 antibody (M1) binding, we label M1 antibody with Cy5 succinimidyl ester (GE Health Care) and purify

it with a gel filtration column. The concentration of M1 is calibrated by measuring the absorption at 280 nm. 500 µL of infected SF9 cell culture is pelleted, washed with Dulbecco's phosphate-buffered saline containing Ca^{2+} and Mg^{2+} (DPBS/Ca, Invitrogen), pelleted again, and then added to 25 µL of lysis buffer containing 20mM HEPES (pH 7.5) and 1 wt% DDM. After 10 min, 25 µL of 40 nM of Cy5-M1 in a buffer containing 20 mM HEPES (pH 7.5) and 2 mM $CaCl_2$ is added to the cell lysate. The binding between M1 antibody and the FLAG tag requires Ca^{2+}. 10 min later, The Cy5-M1/β_2AR mixture is then separated in a "double-T" channel that has the same configuration as described previously in section 4. The separation buffer contains 20 mM HEPES (pH 7.5), 0.1 wt% DDM, 0.02 wt% SDS and 1 mM $CaCl_2$. Laser induced fluorescence detection is achieved using cylindrical optics and a PMT. The concentration of β_2AR is calculated by multiplying the fraction of integrated fluorescence in the β_2AR peak with total M1 concentration (Fig. S5).

For single cell analysis, SF9 cells are harvested 18 hr after infection, washed with DPBS/Ca and adjusted to a final density of about 1 million cells per ml. The analysis using the single-cell microfluidic chip is shown in Fig. 1. Briefly, the cell suspension is injected into the chip using 3 psi of pressure. Valve 1 opens and closes until a cell is close to the three-state valve. The three-state valve then opens to introduce the cell into the reaction chamber. After the three-state valve partially closes, a low pressure is added to the air inlet through valve 2 and valve 5 to remove excess DPBS/Ca. The three-state valve fully closes before filling the channel with lysis/labeling buffer (20 mM HEPES,

pH 7.5, 20 nM Cy5-M1, 1 wt% DDM, 1 mM $CaCl_2$) through valve 6. The three-state

valve partially opens to inject the lysis/labeling buffer into the reaction chamber. Valve 2

closes to confine the volume of injection, and the reaction chamber is filled because of

the air permeability of PDMS. We then fully close the three-state valve to incubate the

cell with the lysis/labeling buffer for 10 min. At the same time, separation buffer (20 mM

HEPES, pH 7.5, 0.1 wt% DDM, 0.02 wt% SDS, 1 mM $CaCl_2$) is injected through valves

3 and 7 to rinse the channels. After the lysis/labeling reaction is complete, a voltage of

1000 V is applied to the chip through valve 7, partially opened three-state valve, valve 2,

and valve 4. The image acquisition starts 20 sec later and an integration time of 20 ms per

frame is used. We lower the voltage to 100 V after the unreacted M1 peak passes the

molecule counting section (~ 46 sec after the separation starts).

6. Culture of *Synechococcus*

The cyanobacterium *Synechococcus sp.* PCC 7942 (*Synechococcus* hereafter) is

grown in BG-11 medium (*S3*) at 30 °C, illuminated at 130 μmol m^{-2} s^{-1} by incandescent

bulbs, and bubbled with 3% CO_2 in air. The –N culture is deprived of nitrogen-containing

nutrients in a way that is similar to the method described before (*S4*). After 72 hr of

nitrogen starvation, the cell culture is harvested and analyzed.

7. Electrophoretic separation of *Synechococcus* lysate

Because of their cell walls, cyanobacteria are much more difficult to lyse than

mammalian cells and insect cells. Traditional ways to lyse cyanobacterial cells use strong

mechanical forces, such as high pressure (French press) or glass bead grinding (bead beater), both of which are difficult to integrate into a PDMS microchip design. We have developed a method to lyse *Synechococcus* cells chemically. 100 to 1000 µL of *Synechococcus* culture is pelleted by centrifugation in a microcentrifuge and then washed with 50 µL HEPES buffer (20 mM HEPES, pH 7.5). After centrifugation, the cell pellet is mixed with 50 µL 10 mg/ml lysozyme in HEPES buffer. After 10 min of incubation at 38 °C, it is washed again with 50 µL HEPES buffer and then mixed with 50 µL or 100 µL B-PER II (Pierce Biotech). Centrifugation after one hour at room temperature results in a blue-green (normal culture) or yellow (nitrogen-depleted culture) cell lysate. Because of the low ionic strength in B-PER II (20 mM Tris, pH 7.5), the phycobilisome degrades to produce smaller phycobiliprotein complexes during the lysis procedure. We have found that lysozyme treatment alone does not release pigments from a cell. On the other hand, after 2 hr or longer treatment with B-PER II, centrifugation results in colorless cell debris and a supernatant showing almost the same blue-green color as the cell suspension before lysis, indicating near complete extraction of the pigment molecules. A freeze-thaw cycle between the lysozyme and B-PER II treatments can shorten the time required for lysis to less than 1 hr by weakening the cell wall.

The cell lysate is diluted at least ten fold into a sample buffer that contains 20 mM HEPES (pH 7.5), 0.1 wt% DDM and 0.012 wt% SDS before it is added to the sample reservoir of a "double-T" chip (same dimension as shown in Fig. S3A). The other three reservoirs are filled with the separation buffer, which contains 20 mM HEPES (pH 7.5),

0.1 wt% DDM and 0.045 wt% SDS. The distance between the injection junction and the detection point is 23 mm. Continuous runs of the separation do not show significant changes in peak heights. This observation indicates that the phycobiliprotein complexes are stable in the sample buffer, but a further increase of the SDS concentration results in gradual dissociation of these protein assemblies.

The identification of the CE separation peaks is facilitated by measuring their fluorescence spectra, which are recorded by the intensified CCD camera on the same microcope. We modify the detection path by inserting a pair of relay lenses and a grating between the microscope and the camera and by placing a 50 μm wide slit at the image plane of the microscope. This modification allows the CCD camera to record wavelength information. Because phycocyanin emission overlaps with the 638 nm laser, we use the 532 nm laser as the excitation source and a dichroic mirror (565DRLPXR, Omega) and a long pass filter (565ALP, Omega) in the emission path. The transmission curves of the filters are calibrated against white light illumination, and the wavelengths in the CCD images are calibrated with the two laser lines.

By comparing the fluorescence spectra with that in the literature (*S5*), and by monitoring the change in the electropherogram when adding different antibodies against phycobiliproteins and linker polypeptides, we are able to identify the major peaks in the electropherogram (See Table S1). Briefly, peaks 2 and 3 are allophycocyanin complexes from the phycobilisome core; peak 6 has both allophycocyanin and phycocyanin; peaks 1,

4, 5, 7, 8, and 9 are phycocyanin complexes associated with various linker polypeptides; and peak 13 is from chlorophyll *a* in photosystem II.

We have also observed that emission spectra of the major peaks in the electropherogram of nitrogen-starved cell lysate matches those from normal cells, which suggests that these peaks have the same contents.

8. *Synechococcus* analysis procedure

The lysis and analysis of individual *Synechococcus* cells is performed on a Nikon TE2000-U inverted microscope using the single-cell analysis chip having three reaction chambers (Fig. 3B). The analysis procedure has three steps (Fig. S5A):

(1) Cell capture. *Synechococcus* cells are treated with lysozyme, washed, diluted into B-PER II, and immediately delivered to the chip from the cell inlet. With a negative pressure applied at the cell outlet by a syringe, the cells flow through one of the reaction chambers. The valves of the reaction chamber are opened and closed randomly. At the same time, phycobiliprotein fluorescence (650 nm - 700 nm) is continuously monitored by imaging through a 40x objective using wide-field illumination with the 636 nm laser. When the valve closes, if no cell or more than one cell is captured, the valve is opened to let the cell suspension continue to flow. Once an individual cell is trapped, the next reaction chamber is moved into the view field and the capturing operation is repeated. It

takes less than 2 min to capture three cells after they are mixed with B-PER II; therefore, no cells are broken during the capture process.

(2) Cell lysis and chip cleaning. After capture, a fluorescent image of each cell is acquired every 10 min to monitor lysis. The excitation light is controlled by a shutter that is synchronized with the CCD acquisition, so that adverse effects (such as photobleaching) are minimized. While the cells are lysing, voltages are applied to wash out the B-PER II solution in the channels (from separation buffer inlet to cell outlet, and then from separation buffer outlets to cell inlet). After all the cells are lysed, the reservoirs are refilled with fresh separation buffer and the chip is washed again.

Fig. S5B shows a fluorescence image sequence of a *Synechococcus* cell. The cell fluorescence initially increases, most likely because of detachment of PBS from thylakoid membranes and their partial dissociation. This disruption of the PBS stops energy transfer to reaction centers with concomitant increased fluorescence from membrane-dissociated PBP complexes. After 50 min, fluorescence from the cell rapidly decreases, reaching a very low level after 70 min. A comparison of the cell fluorescence intensity at 50 and 70 min following exposure to B-PER II indicates the release of more than 90% of the fluorescent cell contents into the reaction chamber.

(3) Separation. To start the separation, we change the excitation path from wide-field configuration to cylindrical configuration, switch from the 40x objective to a 100x

1.4 NA oil immersion objective, and move the view field to the detection point in one of the separation channels. The valves of the corresponding reaction chamber are then opened and a 1000 V separation voltage is applied simultaneously. In single molecule counting, the separation voltage is lowered to 100 V at 18.5 sec after the separation starts. The image acquisition starts at the same time when the voltage is lowered, and the integration time of the ICCD is 50 ms per frame. Cell lysate in the other two reaction chambers are analyzed sequentially.

After the separation step, the next set of cells can be introduced into the reaction chambers for re-initiation of step (1). Thus, the single-cell analysis chip can be used repeatedly, although more than 8 hr of continuous usage could cause degradation in the resolution of CE separation.
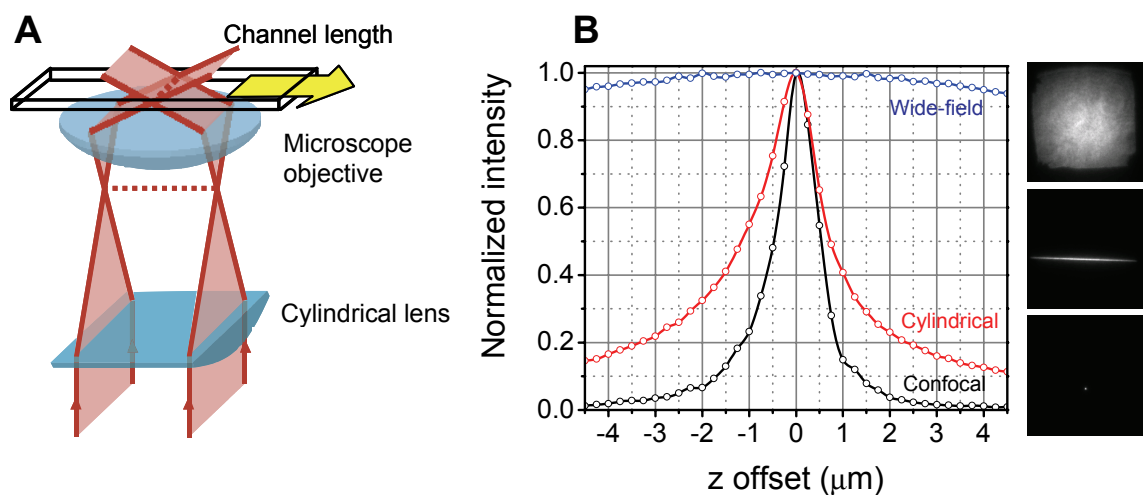
Fig. S1. Creation of the detection curtain. **(A)** Layout of the cylindrical optics. **(B)** *z*-dependence of detected fluorescence from a glass surface coated with Atto 565 labeled streptavidin (Sigma-Aldrich). The fluorescence intensity for the wide-field configuration is measured by averaging a 20 pixel $\times$ 20 pixel area at the center of the view field; the fluorescence intensity for the cylindrical configuration is measured by averaging 20 continuous pixels horizontally aligned at the middle of the focus line; and the fluorescence intensity for the confocal configuration is characterized by the intensity of the pixel at the focal point. The range of *z* that is covered by the molecule counting channel is marked by green dashed lines.
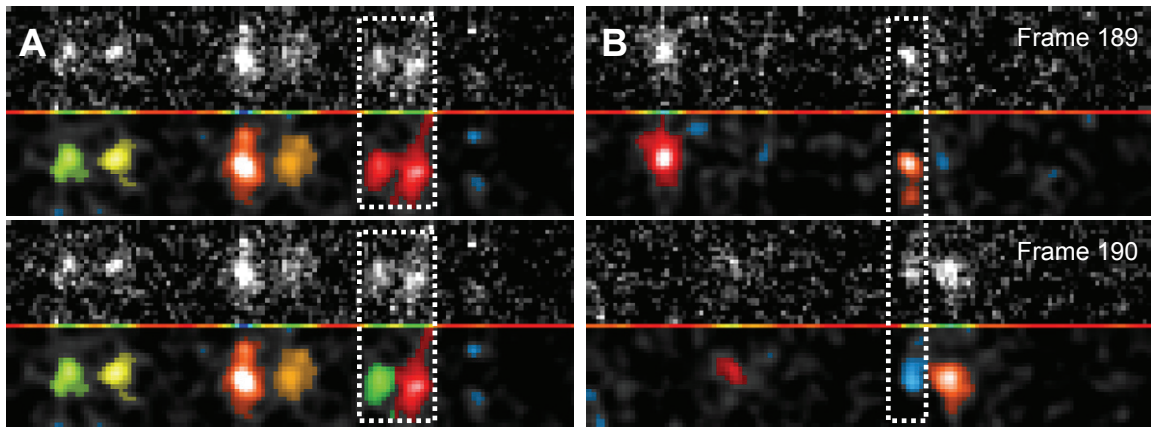
Fig. S2. Image analysis procedure for the separation and counting of A647-SA molecules. In each panel, the upper part is the original image recorded by the CCD camera, the lower part is the image after Fourier filtering, and the colored line between them shows the cross-section of the Fourier filtered image along the detection curtain. In the lower parts, colored regions mark the pixels that are brighter than the threshold. The regions not identified as valid molecule counts appear blue. **(A)** Note the improvement in identification when overlapped fluorescent spots can be split (lower panel). **(B)** When one molecule is imaged in two consecutive frames, the fluorescent spot has the same x position in both frames.
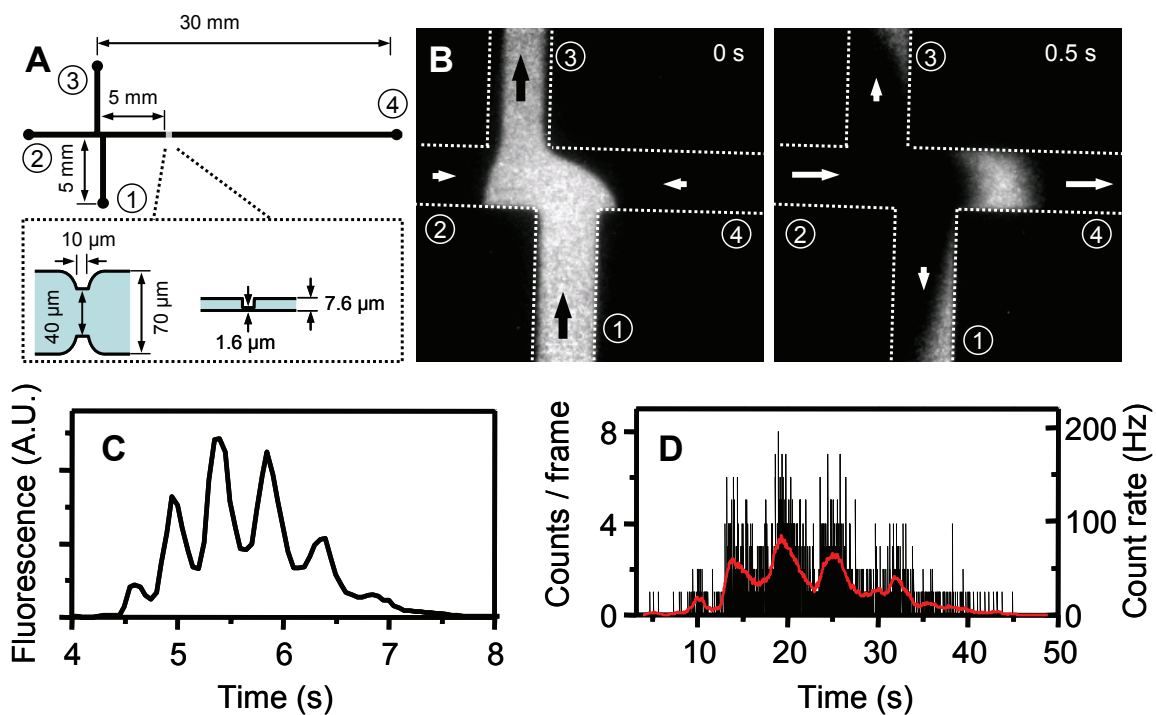
Fig. S3. Analysis of A647-SA in a double-T chip. **(A)** Layout of the "double-T" chip for A647-SA separation. **(B)** Fluorescence images of the double-T junction when separation starts. Dotted lines show the outline of the channels. Timing starts when the voltage set applied to the chip is switched from loading (1 = 1000 V, 2 = 700 V, 3 = 0 V, and 4 = 1000 V) to separation (1 = 700 V, 2 = 1000 V, 3 = 700 V, and 4 = 0 V). Arrows indicate the flow direction. **(C)** CE separation of 100 nM A647-SA. **(D)** Molecule counting of 73 pM A647-SA by lowering the voltage to 1/10 of the ordinary values when the analyte passes the detection curtain, showing the number of identified molecules in each frame of image (black bars) and the average molecule count rate in one-second time bins (red line).
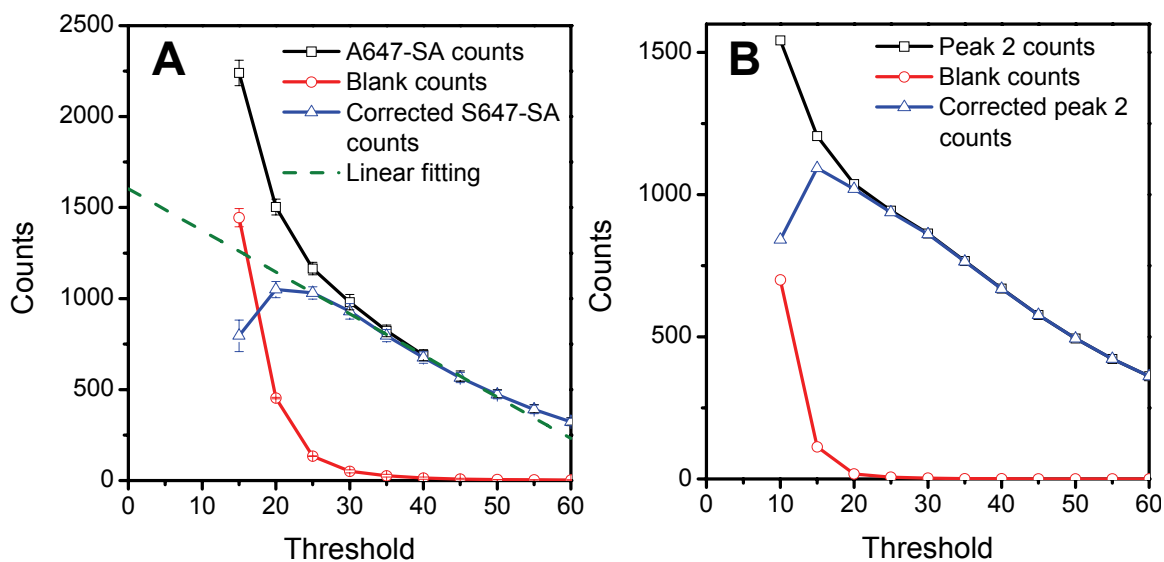
Fig. S4. The dependence of molecule counts on the threshold. **(A)** Counting of A647-SA molecules. The error bars in A647-SA counts are the standard deviations of seventeen measurements, and those in blank counts are the standard deviations in three measurements. **(B)** Molecule counts in peak 2 in cell (c) of Fig. 4B. The blank control is measured in the same chip with no separation voltage applied.
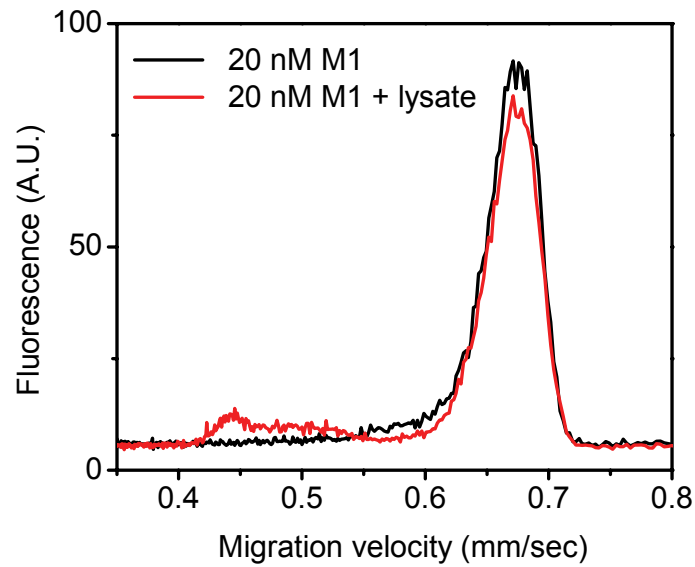
Fig. S5. Electrophoretic analysis of SF9 lysate reacted with excess amount of Cy5-M1.
The *x* scale is converted to the migration velocity, which corresponds to the displacement
along the separation channel of different species at a certain time, so that the integral
reflects the total amount of separated analytes.
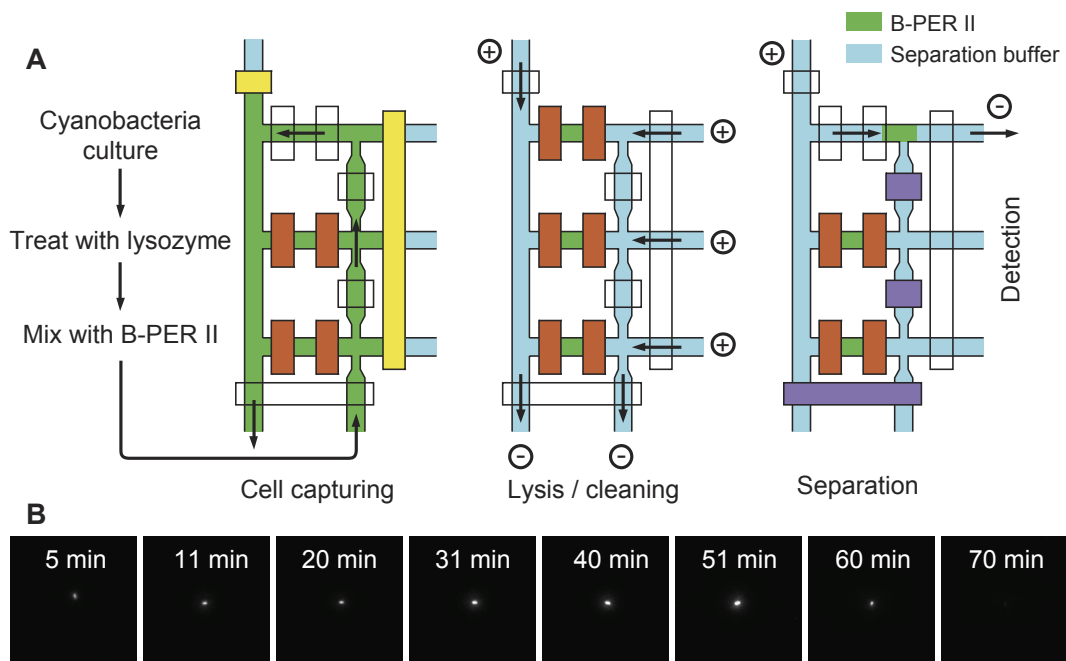
Fig. S6. Analysis of individual cyanobacteria cells. **(A)** Operation procedure of cell capturing, lysis and analysis. **(B)** Fluorescence images of a *Synechoccocus* cell captured in the reaction chamber at different times during the lysis procedure.

Table S1. Emission maxima and identities of major peaks in the

electropherogram of *Synechococcus* lysate.

Peak	Emission maximum (nm)	Chromophore containing protein	Linker peptide[a]	Reported emission maximum (nm)[b]
1	644	PC	L_R^{30}	643
2	680	APC	L_{CM}^{75}	680
3	664	APC	$L_C^{10.5}$	662
4	646	PC	Undetermined	
5	657	PC	Undetermined	
6	654, 679	18S particle (*S5*)	$L_{RC}^{27} + L_{CM}^{75}$	654, 680
7	649	PC	L_R^{33}	648
8	647	PC	None	646
9	652	PC	L_{RC}^{27}	652
12	635, 682	phycobiliprotein monomers[c]		
13	679	Chlorophyll complex		

[a] The denotations of the linker peptides are the same as those in (*S6*).

[b] Data from (*S5*), (*S7*) and (*S8*).

[c] Overlapped with peak 13.

References

S1. H. Wu, A. Wheeler, R. N. Zare, *Proc. Nat. Acad. Sci. U.S.A.* **101**, 12809 (2004).

S2. J. M. Gao, M. Mammen, G. M. Whitesides, *Science* **272**, 535 (1996).

S3. M. M. Allen, *J. Phycol.* **4**, 1 (1969).

S4. J. L. Collier, A. R. Grossman, *J. Bacteriol.* **174**, 4718 (1992).

S5. A. N. Glazer, D. J. Lundell, G. Yamanaka, R. C. Williams, *Ann. Inst. Pasteur Mic.* **B134**, 159 (1983).

S6. A. R. Grossman, M. R. Schaefer, G. G. Chiang, J. L. Collier, *Microbiol. Rev.* **57**, 725 (1993).

S7. D. J. Lundell, R. C. Williams, A. N. Glazer, *J. Bio. Chem.* **256**, 3580 (1981).

S8. D. J. Lundell, A. N. Glazer, *J. Bio. Chem.* **258**, 902 (1983).